Layer relaxation and intermixing in Fe/Cu(001) studied by surface x-ray diffraction

H. L. Meyerheim,* R. Popescu, D. Sander, and J. Kirschner
Max-Planck-Institut für Mikrostrukturphysik, Weinberg 2, D-06120 Halle, Germany

O. Robach and S. Ferrer
European Synchrotron Radiation Facility (ESRF), BP-220, F-38043 Grenoble, France
(Received 26 July 2004; published 18 January 2005)

The structure of Fe films thermally deposited on Cu(001) was analyzed using surface x-ray diffraction in the coverage range between 6 and 8 monolayers. Based on the analysis of crystal truncation rod data measured at 120 and 300 K, i.e., below and above transition temperatures reported for ferro- and antiferromagnetic ordering, no changes of the interlayer spacings larger than about ±0.015 Å are found. Within the Fe film these correspond to fcc Fe (1.78 Å), while the top-layer spacing is expanded by 3–5 % in agreement with previous low-energy electron diffraction studies. Lateral disorder of surface atoms as described by the Debye parameter indicates displacements of the top-layer positions up to 0.23 Å corresponding to zigzag displacements observed in the *p*2*mg* (2×1) superstructure. The inherent large penetration depth of the x rays also allowed the study of the structure and composition of the buried Fe/Cu interface. The data indicate Fe-Cu intermixing, where nearly 50% of a Fe (Cu) monolayer are exchanged. Four layers across the interface are significantly affected. About 30% of the first Fe (Cu) and up to 15% of the second Fe (Cu) layer is alloyed by Cu (Fe).

DOI: 10.1103/PhysRevB.71.035409 PACS number(s): 68.35.Ct, 61.10.−i

I. INTRODUCTION

After more than one decade of intense experimental and theoretical research the structure of Fe deposited on Cu(001) and its correlation to the magnetic properties becomes more and more clear, although some details are still under dispute. Based on experimental[1–19] and theoretical studies,[1–26] consensus has been reached that for Fe films deposited by thermal deposition on Cu(001) at room temperature (RT) three different coverage regimes exist with distinctly different structural and magnetic properties. These are commonly referred to as the ferromagnetic (FM) regime (I) up to about 4 monolayers (ML) $(1\ \text{ML} \coloneqq 1.53\times10^{15}\ \text{atoms/cm}^2)$, where the whole film is FM with a magnetization direction normal to the film plane. Between about 5 and 10 ML regime (II) follows, which is characterized by a FM "live layer" above an antiferromagnetic (AF) stack of layers, which is suggested to adopt a Fe-fcc-like structure. The top layer spacing is reported to show a significant expansion in the order of 5% over the fcc Fe spacing ($d=1.78$ Å).[7–9,11,18] At higher coverage, regime (III) follows, which is characterized by FM bcc Fe, where the easy magnetization axis is in plane in contrast to the regimes (I) and (II), where it is out of plane.

In the recent past, scanning tunneling microscopy (STM) has significantly contributed to the detailed understanding of the relation between structure and magnetism in Fe/Cu(001).[14,15,18,19] It has been shown that in both regimes, (I) and (II), the FM order of the whole film and the top layer is related to the instability of the fcc structure against a monoclinic shear deformation leading to a bcc-like (110) surface layer. This structure is referred to as "nanomartensitic," since it bears close similarity to the fcc-bcc transition in bulk Fe. While in regime (I) the whole film is affected, only the top layer is reported to exhibit the nanomartensistic structure in regime (II). In the context of a hard sphere atomic model, the observed expansion of the interlayer spacings in regime (I) leading to the tetragonal expansion (fct) of the Fe film and the top layer expansion in regime (II) are a natural consequence of the lateral Fe displacements.

Dispute still exists about the detailed magnetic nature of the film in regime (II). In general, theory suggests collinear spin structures, preferentially with a FM coupled bilayer at the free surface.[21,24–27] Especially in the case of an even number of layers (4,6,8 ML) a bilayer AF structure was proposed. And, most important for this structure analysis, a correlation between the character of the interlayer coupling (FM or AF) with the interlayer spacing (expanded or contracted by several percent) was inferred.[21]

At some variance with these models, temperature-dependent (75−300 K) magneto-optic Kerr-effect (MOKE) data collected in the coverage range between 6 and 9 ML could only be interpreted by a spin density wave (SDW).[16] In this model the *top three layers* are always FM coupled, while a SDW with a wave vector $q=(2\pi)\times(0,0,0.37)$ characterizes the magnetic structure of the deeper layers.

With regard to the theoretically predicted correlation between interlayer coupling (FM vs AF) and interlayer relaxation (expanded versus contracted), one may expect that the determination of the interlayer spacings helps to provide additional information on the magnetic structure of thermally deposited Fe/Cu(001). One result of this study is that depending on temperature (i.e., above and below $T_C \approx 250-300$ K for FM ordering and $T_N \approx 200$ *K* for AF ordering within the interior of the film[17]) we do not find obvious evidence for any changes of the interlayer spacings larger than our experimental accuracy of about 0.015 Å.

In general both experimental and theoretical results are commonly discussed and interpreted in terms of an atomically flat and pure Fe film. On the other hand, STM and ion-scattering experiments carried out after deposition of

submonolayer amounts of Fe at room temperature[3,5,27–30] have revealed that interface intermixing occurs in Fe/Cu(001). A recent theoretical study for Fe/Cu(001) by Longo *et al.*[31] supported the experimental observation of submonolayer Fe inclusions,[5,29] indicating that the exchange barrier is reduced for Fe incorporation close to embedded Fe islands.

It should be noted that interface mixing is not limited to the Fe/Cu interface but has been found to be a general phenomenon, which is observed in a number of systems,[32–35] even when no bulk alloy phases are known.[36] Theory also indicates a considerable dependence of the magnetic properties on the interface structure and the degree of intermixing.[37,38] For Fe/Cu it has been found that interdiffusion dramatically reduces the magnetic anisotropy energy (MAE) of the interface layer, making its contribution almost negligible if 30% of Cu is incorporated into the first Fe layer.[37] Recent *ab initio* calculations by Stepanyuk *et al.*[39] on magnetic 3*d* adatoms on Cu(001) show that—although intermixing is energetically favorable—magnetism tends to stabilize the adatom position. From the experimental point of view, different easy magnetization directions of thermally deposited (TD) and pulsed laser deposited (PLD) Fe films on Cu(001) were explained by different interface structures in these system.[40] In contrast to TD films, where the easy axis is out-of-plane up to about 10 ML, for PLD grown films an in-plane easy axis is observed up to about 6 ML. Between 6 and about 8 ML an "inverse" spin reorientation from in-plane to out-of-plane takes place.[41–43] The low-energy electron diffraction (LEED) analysis of a 4-ML-thick PLD-grown Fe film[40] indicates a "flat Cu-bulk-like iron interface layer" while an enhanced surface buckling as compared to TD-grown films is determined. These differences were explained, albeit indirectly, in terms of an enhanced degree of interface mixing in the PLD-grown film. However, direct analysis of the alloy concentration was not possible, because of the limited sensitivity of the LEED intensities to the small differences between the scattering powers of Fe and Cu.

Thus, in spite of the importance of the intermixing problem for the growth, structure, and magnetic properties, little is known on a quantitative basis. As an example, STM experiments are only capable of probing the outermost exposed layer, but do not provide information on the buried interface after several adlayers were grown. LEED is basically able to overcome this problem, but in addition with the comparatively difficult multiple scattering data analysis it probes the near-surface region only due to the limited penetration depth of the electrons. Consequently, its sensitivity to the deeper layers decreases with increasing film thickness. Due to the large x-ray penetration depth and the applicability of single scattering theory, surface x-ray diffraction (SXRD) is a powerful technique for the study of thicker films deposited on a single crystal substrate. To this end we have carried out a SXRD study on the structure of Fe films thermally deposited on Cu(001) at room temperature in the coverage regime between 6 and 8 ML.

II. EXPERIMENT

The experiments were carried out at the beamline ID3 of the European Synchrotron Radiation Facility (ESRF) in Grenoble using a six-circle ultrahigh-vacuum diffractometer operated in the z-axis mode at a wavelength of 0.73 Å.[43] The Cu(001) crystal was cleaned by standard methods of Ar-ion bombardment and subsequent annealing (800 K) until Auger electron spectroscopy (AES) did not show any traces of residual contamination. Fe deposition on the Cu(001) crystal at 300 K was carried out by evaporation from a thoroughly degassed Fe rod heated by electron bombardment. The amount of deposited Fe could be controlled with high accuracy by simultaneous monitoring of a reflection intensity from the Cu(001) crystal close to the (antiphase) (100) position (see below).[44]

In total 7 SXRD data sets (three for 6 ML, two for 7 ML, and two for 8 ML Fe coverage) were collected by measuring the intensity distribution along integer-order crystal truncation rods[45] (CTR) up to a maximum normal momentum transfer of $q_z/c^*=3.2$ reciprocal lattice units (r.l.u.), where $c^*=(2\pi/3.616\ \text{Å})=1.738\ \text{Å}^{-1}$ references the Cu lattice.

Integrated intensities were measured by rotating the sample about its surface normal. In order to avoid systematic errors due to even small sample misalignments, the x-ray incidence angle was chosen to 2°, i.e., significantly above the critical angle of total reflection ($\alpha_c \approx 0.15°$). The smoothness of the Cu crystal and the high-brilliance x-ray beam allowed the collection of reflection curves characterized by a peak intensity of the order of 10^4 counts per second and a full width at half maximum of 0.05° at (1 0 0.1), i.e., close to the antiphase scattering condition.

The structure refinement was carried out by weighted least square fit to the $|F_{obs}|$, allowing the *z* parameters and the Debye parameters ($B=8\pi^2\langle u^2\rangle$, with $\langle u^2\rangle$ the mean square displacement) for each Fe layer and for the first 7 Cu layers from the interface to vary. For a 7-ML sample this adds up to a total of 28 parameters plus an overall scale factor and 2 independent occupancy parameters characterizing the Fe (Cu) concentration in the two Cu (Fe) layers next to the interface if intermixing is taken into account. The ratio between the number of reflections and parameters is about 7, which for SXRD studies is a reasonable value to develop reliable structure models.

III. RESULTS

Figure 1 shows the time dependence of the (10 0.1) intensity during Fe deposition. Pronounced oscillations are observed, where each maximum corresponds to the filling of a complete layer. These are labeled by the numbers. The missing first maximum indicates double layer growth during deposition of the first two layers where interface mixing was observed.[5,29] The growth of subsequent layers proceeds in an almost complete layer-by-layer mode. Since SXRD intensities can be analyzed by single-scattering theory it is possible to quantitatively interpret the data displayed in Fig. 1.

For pseudomorphic growth the (100)-reflection intensity is given by $I(100)\propto|f_{\text{Cu}}/2-\theta f_{\text{Fe}}|^2$, where f_{Cu} and f_{Fe} are the atomic scattering factors of Cu and Fe, respectively, and θ represents the Fe coverage expressed in ML. Since the scattering factors of Cu and Fe differ by 20% only [$f_{\text{Cu}}\approx 24$, $f_{\text{Fe}}\approx 20$ for the (100) reflection[46]], at half-filled layers

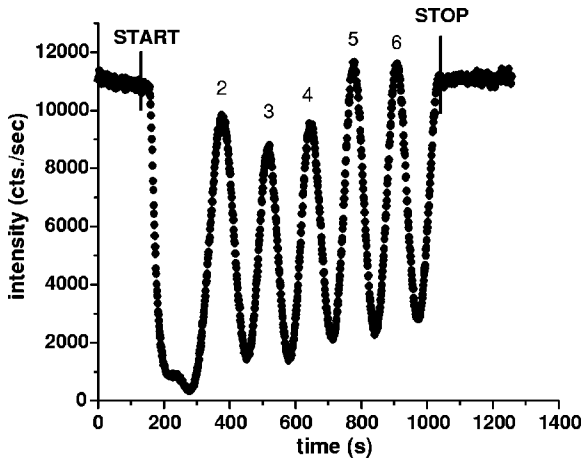

FIG. 1. Reflection intensity at the (10 0.1) position during deposition of Fe on Cu(001) at room temperature. Maxima correspond to the filling of the layers as indicated by the numbers. The missing first maximum indicates double layer growth at the beginning of the deposition.

(θ=0.5) the scattered intensity should be only a few percent of the intensity scattered from the clean Cu(001) surface. Figure 1 shows that in the experiment this prediction is approximately fulfilled. Minima correspond to about 20% of the initial intensity, while the maximum intensity at complete layer filling (θ=1) is almost completely recovered. In this experiment the evaporation was stopped after the seventh maximum. Similarly, Fe films of 6 and 8 ML thickness were prepared. Previous experiments using reflection high-energy electron diffraction (RHEED) and STM have shown that atomically flat Fe films can be grown in this coverage regime, which is a prerequisite for the conclusive analysis of the magnetic properties.[17]

In Fig. 2 the CTR's for 7-ML Fe/Cu(001) measured at RT are shown as a representative example for all data sets. Symbols represent the structure factor amplitudes ($|F_{obs}|$) obtained from the integrated intensities after correcting for apparative factors.[47,48] Standard deviations (σ) of the $|F|$ values are derived from the counting statistics and the reproducibility of symmetry-equivalent reflections.[49,50] In general, error bars are about the size of the symbols in Fig. 2.

In total 364 reflections were collected, reduced to 213 by symmetry equivalence. Based on 151 reflections, where symmetry-equivalent reflections were measured, the average agreement factor equals to 7.9%, which for SXRD studies is a good value. Similar numbers also apply for the other data sets. For the collection of each data set a completely new preparation was carried out. The data discussed in the following were taken during two different experimental runs using two different Cu(001) specimens.

In all cases high-quality data fits could be achieved. The calculated $|F|$'s as represented by the solid lines in Fig. 2 follow the measured ones very closely. All details of the fine oscillations due to the interference of the different layers in the film are correctly described, both in amplitude and phase. The fit quality is quantified by the weighted and unweighted residual,[51,52] which is in the range of 4–7 %. The goodness-of-fit (GOF) parameter[51] is in the 0.8–1.2 range for all data sets.

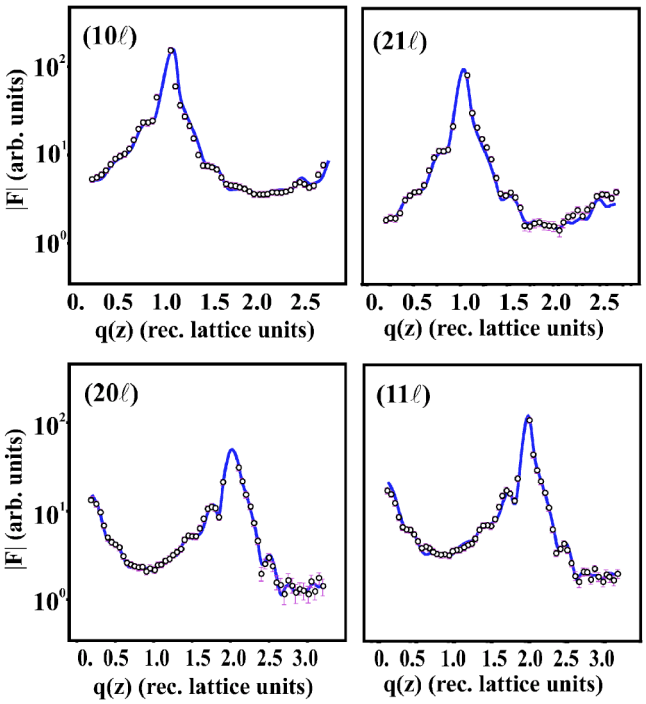

FIG. 2. (Color online) Experimental (symbols) and calculated (lines) structure factor amplitudes for 7-ML Fe/Cu(001) measured at room temperature.

In order to check also the unambiguousness of the results, different starting models (using different layer spacings) were used. These tests confirmed that the best fit could be obtained only by one particular sequence of layer spacings and *B* factors. Thus, we are confident that the results discussed in the following are unambiguous, which is supported by the satisfying reproducibility of the refined structure parameters.

A. Layer relaxation and disorder

Figure 3 compares the interlayer spacings (d_{ij}) derived from the fits to the data sets of the 6-ML (a), 7-ML (b) and 8-ML (c) samples. Cu and Fe layers are numbered from 1, corresponding to the deepest Cu layer (=ninth layer from the interface), up to 17, corresponding to the top Fe layer in the case of the 8-ML sample. The Fe/Cu interface is located between layer 9 (top Cu layer) and 10 (first Fe layer), as shown in the schematic structure model on the right. The corresponding interface distances are labeled by the arrows. All data points representing the interlayer spacings are located between the corresponding layer numbers. Top-layer spacings are emphasized by the rectangles. Horizontal dashed lines represent the layer spacings for fcc Cu (1.808 Å) and fcc Fe (1.78 Å). Data corresponding to samples measured at 300 and 120 K are represented by squares and circles, respectively. Two independent 120-K data sets were measured for 6 ML, corresponding to the two sets of circles shown in Fig. 3(a). Note that two RT data sets were taken for the 7-ML film. Since the results closely coincide only one is shown in Fig. 3(b).

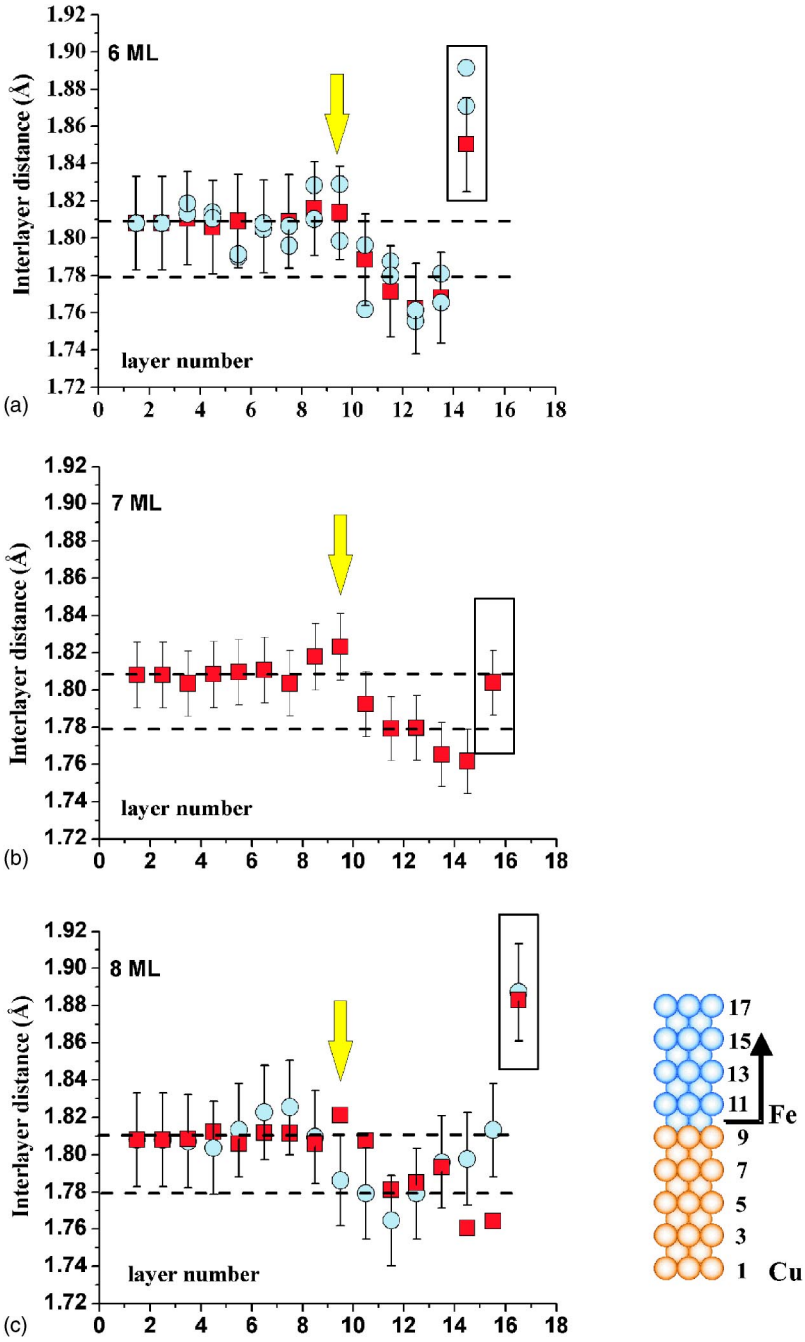

FIG. 3. (Color online) Interlayer spacings given in Å for Fe/Cu(001) covered by 6 (a), 7 (b) and 8 (c) ML Fe. Squares (red) and circles (blue) refer to samples measured at 300 and 120 K, respectively. Arrows indicate the interlayer distances at the Fe/Cu(001) interface. Top-layer spacings are emphasized by the rectangles. A schematic structure model is shown on the right.

For the deepest Cu layers (nos. 1 and 2) the z positions were kept fixed at the bulk value, while the z positions of all other layers were allowed to vary. Due to symmetry (plane group $p4mm$) all x and y positions were kept fixed. For clarity in each figure error bars derived from the variance-covariance matrix ($\Delta z \approx \pm 0.025$ Å) are included for one data set only. In general, considering the overall scatter of the (independent) data sets, it seems that this value slightly overestimates the actual uncertainty of the distance determination, which is in the order of 0.015 Å. Several results can be summarized as follows.

(i) Within the Cu crystal the interlayer spacings correspond to the bulk Cu-value to within ±0.015 Å. There is a slight expansion (≈0.01 Å) of the top Cu-layer spacings (i.e., involving layers 6–9), which appears most pronounced for the 6- and 7-ML samples. This enhanced lattice spacing is also observed at the Fe/Cu interface (see arrows). Assuming pseudomorphic growth of Fe on Cu(001) one would expect a spacing at the interface of only 1.78 Å. Here we find $d_{\mathrm{Cu—Fe}} = 1.82 \pm 0.02$ Å, which might be correlated with an alloyed interface as discussed below.

(ii) In the interior of the Fe film the interlayer spacings correspond to within the experimental accuracy of about ±0.015 Å to that in fcc Fe (1.78 Å). The top-layer spacings are expanded by up to 5%. For the 6- and 8-ML samples we find 1.87±0.015 Å and 1.88±0.015 Å (+5%), respectively, while for the 7-ML sample we derive only 1.80 Å (+1%). There seems to be a correlation between the interlayer spacings with the MOKE measurements of Qian *et al.*[16] carried out at 70 K. For 6 and 8 ML a maximum magnetic signal

was found, while for 7 ML the magnetic signal has a minimum. This behavior was explained using a model involving a SDW rather than a collinear AF spin structure. Therefore one could speculate that the top-layer spacings might be related to the magnetic structure, but in order to verify this speculation further investigations are necessary.

All interlayer spacings of the deeper layers and the top-layer expansions are—as far as comparable—in very good agreement with those found in several LEED studies.[7,9,19] For the top spacing, values between 1.83 and 1.89 Å were determined and explained in terms of a hard-sphere model in the context of the shear instability of the top-layer Fe structure. At a coverage of 6 ML, the top layer is reported to form a *p2mg* (2×1) superstructure.[7,9,53] A more recent investigation also reports on a *p4gm* (2×2) superstructure,[19] which is closely related to the *p2mg* (2×1) superstructure in that the zigzag displacements of the surface Fe atoms are running along both lateral directions.

We did not find any evidence for the presence of half-order reflections, most likely because the superstructures are not sufficiently long-range ordered. It should be emphasized that in spite of the insufficient long-range order local shifts of the atomic positions can be analyzed by measuring the CTR intensities, since these are sensitive to the local atomic shifts relative to the (1×1) surface unit cell. The lateral atomic shifts will be discussed below in terms of the Debye parameter.

(iii) Within an accuracy of 0.020 Å we have no evidence for any temperature dependence of the d_{ij}. This is most evident from the 6-ML sample, while for the 8-ML sample the two spacings, $d_{14/15}$ and $d_{15/16}$, appear to slightly expand upon cooling, although the error bars derived from the covariance matrix still overlap. We do not think that this result is physically meaningful, since the overall scatter of the 8-ML data is larger than that in the 6- and 7-ML data sets and the fit quality for the 8-ML data is the worst of all, possibly due to some contamination.

The temperature *independence* of the lattice spacings is an important result, since the low-temperature measurements ($T\approx120$ K) were carried out well below both the FM ordering temperature ($T_C\approx250-300$ K) and the AFM ordering temperature ($T_N\approx200$ K) in this coverage regime.[16,20] Local spin density (LSD) calculations have predicted considerable (up to 5%) expansion and contraction depending on whether the layers are FM or AFM coupled, respectively.[21,25] This is commonly referred to as the "magnetovolume" effect. Thus we have experimental evidence that if there is any dependence of the layer spacings on the magnetic interlayer coupling it is below about ±0.02 Å (±1%).

(iv) Structural disorder as expressed by the Debye parameters B was refined for each layer simultaneously. In the most general case, B describes the displacement of the atoms out of their average positions, which can be dynamic (thermal vibrations) or static (average over an ensemble of displaced atoms) in nature. In the isotropic case the mean square displacement of an atom out of its average position, $\langle u^2\rangle$, is related to B by the relation $B=8\pi^2\langle u^2\rangle$.

Figure 4(a) shows (isotropic) layer-resolved B's for 7-ML Fe/Cu(001) measured at room temperature. Solid squares and circles correspond to structure models involving an abrupt and intermixed Fe/Cu interface, respectively (see below). The B factors for the deepest Cu layers (nos. 1 and 2) were kept at bulk values close to $B=0.6$ Å^2, equivalent to a root mean square (rms) displacement of $\sqrt{\langle u^2\rangle}\approx0.09$ Å.

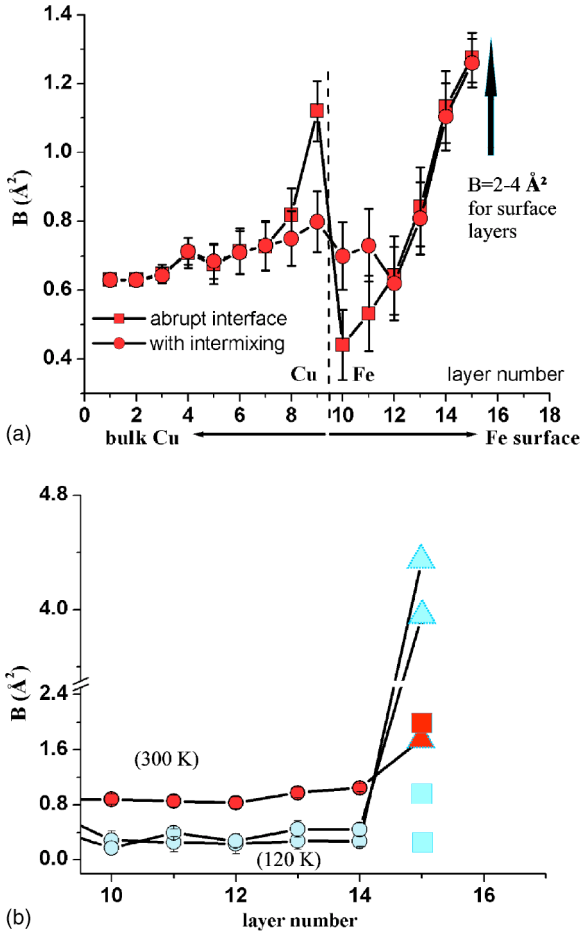

FIG. 4. (Color online) (a) Layer dependent Debye parameter for 7-ML Fe/Cu(001) at RT. Only the B factors for layers in the interior of the film are shown. Squares and circles correspond to structure models assuming an abrupt and intermixed Fe/Cu interface, respectively. (b) Temperature-dependent Debye parameters of Fe layers in 6-ML Fe/Cu(001). Dark (red) and bright (blue) symbols represent 300– and 120-K data, respectively. Circles correspond to isotropic B's. For the top layer, anisotropic B factors parallel ($\parallel$, triangles) and perpendicular ($\perp$, squares) to the surface are shown.

Within the Cu crystal, B is slowly increasing in the direction towards the interface, but across the interface nos. 8–11 we find anomalously enhanced (8,9) and reduced (10,11) values. Allowing for interface alloying within the two Cu and Fe layers at the interface removes the "anomaly," and within the error bars the B_r factors are smooth across the interface as represented by the solid circles. Interface alloying will be discussed in more detail below. In the interior of the Fe film the B factors also increase in the direction towards the surface, although the absolute rms displacement amplitudes are still in the range normally seen in thin films and surfaces. As an example a B value of 1.3 Å^2 for the second Fe layer from the surface (no. 15) corresponds to $\sqrt{\langle u^2\rangle}\approx0.13$ Å. These

numbers can be tentatively attributed to dynamic (thermal) disorder, but a clear discrimination between dynamic and static disorder is only possible by temperature-dependent measurements. In contrast to all layers in the interior of the film as discussed so far, for the top layer [not included in Fig. 4(a)], extremely large B's in the 2.0–4.5-Å^2 range, corresponding to $\sqrt{\langle u^2\rangle} \approx 0.16-0.23$ Å are observed. These can hardly be attributed to thermal vibration amplitudes but must rather be related to static disorder as discussed in the following.

Temperature-dependent measurements were carried out for 6-ML Fe/Cu(001), where also the $p2mg$ (2×1) superstructure is reported to be best ordered.[9] One data set was taken at 300 K and two at 120 K. The results are displayed in Fig. 4(b). Dark (red) and blue (bright) symbols represent room temperature and 120-K data, respectively. For all five Fe layers in the interior of the film (layers 10–14) isotropic B's were refined (circles). The two low-temperature data show very good reproducibility. The larger B's for the 300-K sample prove that in the interior of the film thermal vibrations are the dominant factor contributing to the disorder. An estimation of the temperature dependence of B yields a Debye temperature of $\Theta_D \approx 80-100$ K.

For the topmost Fe layer both large (up to 4–4.5 Å^2) and anisotropic B factors are observed. Therefore, the analysis was carried out by using anisotropic B factors labeled by $B_\parallel$ (triangles) and $B_\perp$ (squares) for the parallel and the perpendicular direction, respectively. Note that for the parallel component a dramatic increase with *decreasing* temperature is observed. This cannot be attributed to dynamic disorder but must be related to static disorder due to lateral atomic shifts. In contrast to the parallel component, the perpendicular B component shows "normal" dynamic behavior.

The large parallel displacement amplitudes are directly related to the lateral shifts of the surface Fe atoms out of the hollow site positions, which have been identified previously on the basis LEED and STM work[15,18,53] and were found to be energetically favorable on the basis of *ab initio* LSD calculations.[25] For instance, Heinz *et al.*[53] find in their LEED analysis of the $p2mg$ (2×1) phase observed at 6 ML an antiparallel 0.2 Å lateral shift (s_D) of the top-layer atoms out of their fcc hollow site positions. This is in good agreement with our results ($\sqrt{\langle u^2\rangle} \approx 0.16-0.23$ Å). Later investigations by Tschielessnig *et al.*[18] derived values between $s_D=0.10$ and 0.14 Å and $s_D=0.06$ and 0.08 Å for the $p4gm$ and $p2mg$ structures, respectively. Our temperature-dependent data [Fig. 4(b)] indicate structural ordering when the sample is cooled from room temperature to 120 K.

Finally, we point out that the s_D's are considerably smaller than observed in STM images for the nanomartensite structure[14] and theoretically predicted.[25] The superstructures [$p2mg$ (2×1) and the $p4gm$ (2×2)] are closely related to the $n=2$ versions of the nanomartensitic $(1\times n)$ superstructures observed at lower coverage. In the nanomartenite needles the shift of adjacent Fe atoms is about 0.6 Å, but in the coverage regime above 4 ML the surface fraction of this structure is at most 10%;[19] therefore the analysis of the scattering data is dominated by s_D related to the (1×2) [or (2×2)] reconstruction.

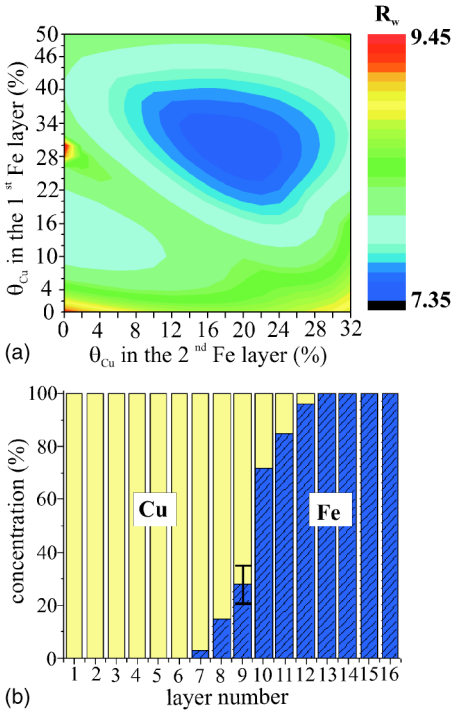

FIG. 5. (Color online) (a) Weighted residuum for 7-ML Fe/Cu(001) versus Cu concentration in the first (θ_1) and second (θ_2) Fe layer. R_w is represented by a color code as shown on the right. Blue (dark) and yellow (bright) correspond to low and high R_w. (b) Schematic view of the concentration profile across the Fe/Cu interface. The average over the results from all data is shown. Bright and dark bars represent the Cu and Fe concentration, respectively. At layer 9 the error bar for the concentration is indicated.

B. Interface alloying

Interface alloying induces a change of the scattering power of the layers. Since Fe (Cu) alloying of Cu (Fe) corresponds to decrease (increase) of the scattering power, this is reflected by an artificially increased (decreased) B factor as shown in Fig. 4(a) if the interface is assumed to be abrupt. In contrast, the positional parameters are not affected within 5×10^{-3} Å by including intermixing into the structure model.

Apart from removing the B factor anomaly at the interface, the agreement parameters[51] are improved if interface intermixing is included in the structure model. As an example, Fig. 5(a) shows for a 7-ML sample the weighted residuum (R_w) versus θ_1 and θ_2, the Cu concentration in the first and second Fe layer, respectively. R_w is shown in a color code, where dark (blue) and bright (yellow) regimes correspond to low and high R_w as shown on the right. Simultaneously, the Fe concentration in the Cu layers was also varied in order to preserve the mass balance across the interface. Structure refinement on the basis of the abrupt interface model [$\theta_1=0$, $\theta_2=0$, lower left corner in Fig. 5(a)] yields $R_w=0.087$, while the best fit at $\theta_1=29\%$, $\theta_2=20\%$ corresponds to $R_w=0.074$, which represents an improvement by about 18%. The GOF parameter drops from 1.38 to 1.20. A similar behavior is also observed for the other 6 data sets. Here the R_w's improve by 10% to 19%. Finally, it should be

added that the unweighted residuum (R_u), which does not include a statistical analysis, behaves in the same way.

In order to check the statistical significance of the improved fit quality we have carried out the *R*-factor ratio test, which was introduced by Hamilton.[52] This procedure is especially important here since the intermixing model involves two additional independent parameters. The test clearly indicates that the improvement of the *R* factor is significant with a probability of more than 99.5%. Thus, we conclude that the SXRD data provide evidence for interface alloying, which significantly affects four layers next to the interface (two Cu and two Fe layers).

For θ_1 and θ_2 we find values in the 22–35 % and 7–22 % range, respectively. Figure 5(b) shows the concentration profile across the interface representing the average results derived from all seven data sets. The bars represent the Cu (bright) and Fe (dark) concentration versus layer number. As in Figs. 3 and 4 the (ideal) Fe/Cu interface is between layers 9 (Cu) and 10 (Fe). The error bars of the concentration determination are in the 5–10 % range as indicated for layer 9. In two cases some intermixing extending up to the third layer from the interface is found, but in these layers the alloy concentration never exceeds a few percent. In total, nearly half a ML of Fe is exchanged with Cu across the interface and vice versa.

Our results are of importance for state of the art calculations concerning the magnetic structure of Fe films deposited on Cu(001). Despite its potential to be a decisive factor for the film magnetism, in general interface alloying has not been considered in detail, although some studies were carried out. These have indicated the impact of intermixing on key properties such as magnetic moments, magnetic anisotropy energy, and magnetic coupling strength.[26,37,39,54–56]

No detailed information on the lateral structural correlations within the alloyed layers can be given, since only the (1×1) CTR's were probed in the SXRD experiments. Experiment and theory support a model of Fe patches embedded in the Cu surface,[5,29,31] but the activation energy for interdiffusion [1.45 eV (Ref. 56), 0.78 eV (Ref. 31)] imposes a kinetic barrier, which prevents substantial alloying, at least at low temperatures.

IV. SUMMARY

In summary, we have carried out an extensive SXRD study of the structure of Fe thermally deposited at RT on Cu(001) in the coverage range between 6 and 8 ML. Based on seven independent data sets, interlayer distances, structural disorder as modeled by the Debye parameter, and interface alloying were analyzed in detail. The reproducibility of the interlayer distance determination was found to lie in the ±0.015-Å range. The inherent large x-ray penetration depth allows the analysis of deeper lying layers and the Fe/Cu interface with no loss of sensitivity. Measurements carried out at 120 and 300 K did not indicate detectable changes of the layer spacings. Since these temperatures are well below and above reported temperatures for FM ($\approx$250–300 K) and AFM ($\approx$200 K) ordering, the correlation of the magnetic ordering with layer spacing is—if present—below our experimental accuracy of 0.015 Å. Analysis of structural disorder indicates substantial lateral disorder for the top Fe layer, which is explained in terms of the zigzag shear displacements of the Fe atoms present in superstructures [$p2mg$ (2×1) and $p4gm$ (2×2)], consistent with previous LEED studies. The high accuracy and sensitivity of the SXRD data allowed the analysis of the interface structure, where interface alloying was determined. Intermixing was found for four layers (two Fe and two Cu) adjacent to the interface. We find that up to about 30% and 15% of the first and second Fe (Cu) layer is alloyed by Cu (Fe), respectively. This analysis is important for theoretical studies of the magnetic ground state of the Fe film in this coverage regime as intermixing is known to modify the magnetic properties.

ACKNOWLEDGMENT

We (H.L.M., R.P., and D.S.) would like to thank the ESRF for hospitality during their stay.

*Electronic address: hmeyerhm@mpi-halle.mpg.de

[1] J. Thomassen, F. May, B. Feldmann, M. Wuttig, and H. Ibach, Phys. Rev. Lett. **69**, 3831 (1991).
[2] M. Wuttig, B. Feldmann, J. Thomssen, F. May, H. Zillgen, A. Brodde, H. Hanemann, and H. Neddermeyer, Surf. Sci. **291**, 14 (1993).
[3] T. Detzel, N. Memmel, and T. Fauster, Surf. Sci. **293**, 227 (1993).
[4] K. E. Johnson, D. D. Chambliss, R. J. Wilson, and S. Chiang, J. Vac. Sci. Technol. A **11**, 1654 (1993).
[5] K. E. Johnson, D. D. Chambliss, R. J. Wilson, and S. Chiang, Surf. Sci. Lett. **313**, L811 (1994).
[6] A. Fuest, R. D. Ellerbrock, A. Schatz, W. Keune, R. A. Brand, and H.-D. Pfannes, Hyperfine Interact. **92**, 1297 (1994).
[7] P. Bayer, S. Müller, P. Schmailzl, and K. Heinz, Phys. Rev. B **48**, 17 611 (1993).
[8] S. Müller, P. Bayer, C. Reischl, K. Heinz, B. Feldmann, H. Zillgen, and M. Wuttig, Phys. Rev. Lett. **74**, 765 (1995).
[9] K. Heinz, S. Müller, and P. Bayer, Surf. Sci. **352–354**, 943 (1996).
[10] M. Zharnikov, A. Dittschar, W. Kuch, C. M. Schneider, and J. Kirschner, Phys. Rev. Lett. **76**, 4620 (1996).
[11] M. Zharnikov, A. Dittschar, W. Kuch, C. M. Schneider, and J. Kirschner, J. Magn. Magn. Mater. **174**, 40 (1997).
[12] J. Shen, C. Mohan, P. Ohresser, M. Klaua, and J. Kirschner, Phys. Rev. B **57**, 13 674 (1998).
[13] R. Vollmer and J. Kirschner, Phys. Rev. B **61**, 4146 (1996).
[14] A. Biedermann, M. Schmid, and P. Varga, Phys. Rev. Lett. **86**, 464 (2001).
[15] A. Biedermann, R. Tscheließnig, M. Schmid, and P. Varga, Phys. Rev. Lett. **87**, 086103 (2001).
[16] D. Qian, X. F. Jin, J. Barthel, M. Klaua, and J. Kirschner, Phys. Rev. Lett. **87**, 227204 (2001).

[17] D. Qian, X. F. Jin, J. Barthel, M. Klaua, and J. Kirschner, Phys. Rev. B **66**, 172406 (2002).
[18] R. Tscheliessnig, A. Biedermann, W. Rupp, M. Schmid M, and P. Varga, in *Proceedings of 7th International Conference on Nanometer-Scale Science and Technology and 21st European Conference on Surface Science* (NANO-7/ECOSS-21), Malmo, Sweden, June 2002 (Lund Univ., Lund, Sweden, 2002).
[19] A. Biedermann, R. Tschelißnig, M. Schmid, and P. Varga, Appl. Phys. A: Mater. Sci. Process. **78**, 807 (2004).
[20] D. Li, M. Freitag, J. Pearson, Z. Q. Qiu, and S. D. Bader, Phys. Rev. Lett. **72**, 3112 (1994).
[21] E. G. Moroni, G. Kresse, and J. Hafner, J. Phys.: Condens. Matter **11**, L35 (1999).
[22] D. Spisak and J. Hafner, Phys. Rev. B **61**, 16 129 (2000).
[23] R. E. Camley and D. Li, Phys. Rev. Lett. **84**, 4709 (2000).
[24] D. Spisak and J. Hafner, Phys. Rev. B **66**, 052417 (2002).
[25] D. Spisak and J. Hafner, Phys. Rev. Lett. **88**, 056101 (2002).
[26] T. Asada and S. Blügel, Phys. Rev. Lett. **79**, 507 (1997).
[27] J. Shen, J. Giergiel, A. K. Schmid, and J. Kirschner, Surf. Sci. **328**, 32 (1999).
[28] D. D. Chambliss, K. E. Johnson, R. J. Wilson and S. Chinag, J. Magn. Magn. Mater. **121**, 1 (1993).
[29] D. D. Chambliss and K. E. Johnson, Surf. Sci. **313**, 215 (1994).
[30] D. D. Chamblis, R. J. Wilson, and S. Chinag, J. Vac. Sci. Technol. A **10**, 1993 (1992).
[31] R. C. Longo, V. S. Stepanyuk, W. Hergert, A. Vega, L. J. Gallego, and J. Kirschner, Phys. Rev. B **69**, 073406 (2004).
[32] D. D. Chambliss and S. Chang, Surf. Sci. Lett. **264**, L187 (1992).
[33] P. W. Murray, I. Stensgaard, E. Lægsgaard, and F. Besenbacher, Phys. Rev. B **52**, R14 404 (1995).
[34] P. T. Sprunger, E. Lægsgaard, and F. Besenbacher, Phys. Rev. B **54**, 8163 (1996).
[35] J. Fassbender, R. Allenspach, and U. Dürig, Surf. Sci. **383**, L742 (1997).
[36] J. Tersoff, Phys. Rev. Lett. **74**, 434 (1995).
[37] B. Ujfalussy, L. Szunyough, and P. Weinberger, Phys. Rev. B **54**, 9883 (1996).
[38] Z. Yang and R. Wu, Surf. Sci. **496**, L23 (2002).
[39] V. S. Stepanyuk, A. N. Baranov, W. Hergert, and P. Bruno, Phys. Rev. B **68**, 205422 (2003).
[40] M. Weinelt, S. Schwarz, H. Baier, S. Müller, L. Hammer, K. Heinz, and Th. Fauster, Phys. Rev. B **63**, 205413 (2001).
[41] J. Shen, H. Jenniches, Ch. V. Mohan, J. Barthel, M. Klaua, P. Ohresser, and J. Kirschner, Europhys. Lett. **43**, 349 (1998).
[42] H. Jenniches, J. Shen, Ch. V. Mohan, S. S. Monoharan, J. Barthel, P. Ohresser, M. Klaua, and J. Kirschner, Phys. Rev. B **59**, 1196 (1999).
[43] S. Ferrer and F. Comin, Rev. Sci. Instrum. **66**, 1674 (1995).
[44] We use a sample setting corresponding to a primitive surface unit cell, where the surface (s) setting is related to the face-centered-cubic setting of the bulk (b) by the following relations: $[100]_s = \frac{1}{2}([100]_b - [010]_b)$; $[010]_s = \frac{1}{2}([100]_b + [010]_b)$, and $[001]_s = [001]_b$.
[45] I. K. Robinson, Phys. Rev. B **33**, 3830 (1986).
[46] *International Tables for Crystallography*, edited by A. Wilson (Kluwer Academic, Dordrecht, 1985), Vol. C.
[47] E. Vlieg, J. Appl. Crystallogr. **30**, 532 (1997).
[48] N. Jedrecy, J. Appl. Crystallogr. **33**, 1365 (2000).
[49] R. Feidenhans'l, Surf. Sci. Rep. **10**, 105 (1989).
[50] I. K. Robinson and D. J. Tweet, Rep. Prog. Phys. **55**, 599 (1992).
[51] The unweighted residual (R_u) is defined as $R_u = \Sigma \| F_{obs} | - | F_{calc} \| / \Sigma | F_{obs} |$, where F_{obs} and F_{calc} are the observed and calculated structure factors, respectively, and the summation runs over all datapoints; similarly, the weighted residual $R_{(u)}$ and GOF are defined by $R_w = [\Sigma w (|F_{obs}| - |F_{calc}|)^2 / \Sigma w |F_{obs}|^2]^{1/2}$; $\mathrm{GOF} = \{[1/(N-P)] \Sigma w (|F_{obs}| - |F_{calc}|)^2\}^{1/2}$, where N and P are the number of reflections and refined parameters, respectively, and $w = 1/\sigma^2$ is weighting factor using the standard deviation (σ) as parameter.
[52] W. C. Hamilton, Acta Crystallogr. **18**, 502 (1964).
[53] K. Heinz, S. Müller, and L. Hammer, J. Phys.: Condens. Matter **11**, 9437 (1999).
[54] D. Spisak and J. Hafner, Phys. Rev. B **56**, 2646 (1997).
[55] S. H. Kim, K. S. Lee, H. G. Min, J. Seo, S. C. Hong, T. H. Rho, and J.-S. Kum, Phys. Rev. B **55**, 7904 (1997).
[56] D. Spisak and J. Hafner, Phys. Rev. B **64**, 205422 (2001).